tvst

https://doi.org/10.1167/tvst.7.5.23

Article

Universal Corneal Epithelial-Like Cells Derived from Human Embryonic Stem Cells for Cellularization of a Corneal Scaffold

Juan Yang[1], Jung Woo Park[1], Dejin Zheng[1], and Ren-He Xu[1]

[1] Center of Reproduction, Development & Aging, and Institute of Translational Medicine, Faculty of Health Sciences, University of Macau, Taipa, Macau, China

Correspondence: Faculty of Health Sciences, University of Macau, Avenida da Universidade Taipa, Macau, China. e-mail: Renhexu@umac.mo

Received: 15 June 2018
Accepted: 7 August 2018
Published: 10 October 2018

Keywords: human embryonic stem cells; differentiation; corneal epithelial cells; decellularized cornea; *B2M* knockout; immunogenicity

Citation: Yang J, Park JW, Zheng D, Xu R-H. Universal corneal epithelial-like cells derived from human embryonic stem cells for cellularization of a corneal scaffold. Trans Vis Sci Tech. 2018;7(5):23, https://doi.org/10.1167/tvst.7.5.23

Purpose: We generated universal corneal epithelial cells (CEC) from human embryonic stem cells (hESC) by genetically removing human leukocyte antigens (HLA) class I from the cell surface.

Methods: The serum-free, growth factor-free, and defined medium E6 was used to differentiate hESC to CEC. Decellularized murine corneas were recellularized with hESC-derived CEC. Using CRISPR/Cas9, *β-2-microglobulin* (*B2M*) was deleted in hESC to block the assembly of HLA class-I antigens on the cell surface to generate $B2M^{-/-}$ CEC.

Results: E6 alone was sufficient to allow hESC differentiation to CEC. A time-course analysis of the global gene expression of the differentiating cells indicates that the differentiation closely resembles the corneal development in vivo. The hESC-CEC were highly proliferative, and could form multilayer epithelium in decellularized murine cornea, retain its transparency, and form intact tight junctions on its surface. As reported before, *B2M* knockout led to the absence of HLA class-I on the cell surface of hESC and subsequently derived CEC following stimulation with inflammatory factors. Moreover, $B2M^{-/-}$ CEC, following transplantation into mouse eyes, caused less T-cell infiltration in the limbal region of the eye than the wild-type control.

Conclusions: CEC can be derived from hESC via a novel and simple protocol free of any proteins, hESC-CEC seeded on decellularized animal cornea form tight junctions and allow light transmittance, and $B2M^{-/-}$ CEC are hypoimmunogenic both in vitro and in vivo.

Translational Relevance: $B2M^{-/-}$ hESC-CEC can be an unlimited and universal therapy for corneal repair in patients of any HLA type.

Introduction

Corneal diseases affect millions of people worldwide. For example, limbal stem cell deficiency (LSCD) is characterized by the loss or deficiency of stem cells in the limbus that are critical for the regeneration of corneal epithelial cells (CEC). Limbal stem cells (LSC) dynamically differentiate into CEC via intermediate progenitor cells, including transiently amplifying cells.[1] Thus, loss or deficiency of LSC will lead to corneal conjunctivalization, chronic inflammation, and potential vision loss after the corneal damage.[2] Although medical management to restore the limbal microenvironment and optimize the ocular surface has some effects at the early stage of LSCD,[3] corneal and LSC transplantation to date have been the most effective treatment method.[4] However, transplantation of autologous LSC risks the healthy cornea of the contralateral donor eye, and allogeneic transplantation is limited by shortage of donors or immunologic incompatibility.[5,6] Interests are rising to seek therapeutic alternatives using CEC derived from human pluripotent stem cells (hPSC), including human embryonic stem cells (hESC)[7] and induced pluripotent stem cells (iPSC).[8,9]

Many protocols have been developed for the

differentiation of CEC from hPSC under conditions that resemble the LSC niche or contain various promoting factors. For examples, CEC are derived from hPSC in a culture medium conditioned by limbal fibroblast or LSC,[10–13] or coculture with PA6 stromal cells as feeder,[14] or on extracellular matrix enriched surface[15] and engineered biomaterials, such as de-epithelialized Bowman's membrane of corneas.[16] Recently, defined media have been used to mimic the conditions in vivo for corneal epithelium specification via constitution of signaling cues, including transforming growth factor β (TGFβ), Wnt, and fibroblast growth factor (FGF) signaling.[17–20]

Efforts also have been explored to seek engineered biomaterials, for example, modified human amniotic membrane, collagen, fibrin, poly(epsilon-caprolactone), silk fibroin-chitosan, and chitosan-gelatin as corneal cell carriers.[20–26] However, they often do not meet the clinic standards for transparency, mechanical strength, biocompatibility, and biosafety. In contrast, decellularized cornea (DC) have emerged as a relatively safe and sustainable scaffold for cell delivery, since it not only maintains the corneal architecture, strength, and optical properties, but also retains native matrix ultrastructure. Recellularization of porcine DC with rabbit corneal cells can build up a sheet of rabbit corneal equivalent.[27] Similar results were obtained with porcine DC recellularized with human corneal cells.[28] In addition, CEC derived from hESC in DMEM/F12 mixed at 1:1 with keratinocyte serum-free medium under 7% O_2 are seeded on decellularized porcine limbal matrix followed by air-lift culture to induce epithelial stratification.[29] Although human DC is a better choice compared to the animal counterparts, as they possess human corneal properties and will not cause xenogeneic immune response,[30] the limited availability of the source still imposes a major hurdle to their use.

Traditionally, the cornea has been considered as an immune privileged site in the body. However, immune rejection remains the leading cause of corneal allograft failure, accompanied by vascularization, inflammation, and corneal graft failure.[31] Thus, disparities in the polymorphic human leukocyte antigen (HLA) molecules between a donor and an allogeneic recipient can elicit immune responses after corneal transplantation.[32] It is difficult to find HLA-matched donors and risky to administrate long-term immunosuppressive agents to recipients of allogeneic cornea. Although iPSC can be derived from a patient and differentiate into CEC,[8,9] which should be immunologically compatible for the treatment of the same patient, it takes a couple of months to reprogram patient's cells into iPSC and differentiate the iPSC into CEC. Besides, it is economically a burden for patients to pay for all of the procedures. To address these problems, scientists have conducted genetic manipulations to generate hPSC without HLA class-I or -II molecules, so-called "universal" hPSC.[33] Allogeneic cells without the surface expression of the HLA molecules become invisible to immune cells of a recipient.[34]

We differentiated hESC into CEC using a simple E6 medium without cytokines and growth factors. The gene expression profile of the differentiating hESC somehow mimics the developmental procedures during the embryonic corneal formation. Moreover, we recellularized murine DC with hESC-derived CEC, which formed multilayered epithelium on the top of the DC with sustained transparency and restored tight junctions. More importantly, we generated hypoimmunogenic CEC by disrupting the nonpolymorphic gene *β-2-microglobulin* (*B2M*) in hESC as reported by others[35-39] except that CRISPR/Cas9 was used here. $B2M^{-/-}$ CEC lost the surface expression of HLA class-I and caused less T cell infiltration than wild-type (WT) CEC after injection into the anterior chamber of immunocompetent mice.

Methods

Ethics Approval and Consent to Participate

Human embryonic stem cell lines were used in this study in accordance with the National Institutes of Health (NIH; Bethesda, MD) Guidelines on Human Stem Cell Research. Animal use and care protocol was approved by the University of Macau Ethics Panel.

hESC Culture in E8 and Differentiation into CEC in E6

hESC were cultured on Matrigel-coated culture plates in E8 medium (Invitrogen, Carlsbad, CA) and routinely passaged every 3 to 4 days with ethylenediaminetetraacetic acid/Dulbecco's phosphate buffered saline (EDTA/DPBS).[40] The following hESC lines were used in this study: H1, H9,[7] CT3,[41] and Envy (GFP^+) derived from hES3.[42]

For differentiation into CEC, hESC were split with EDTA/DPBS as small clumps in a culture plate

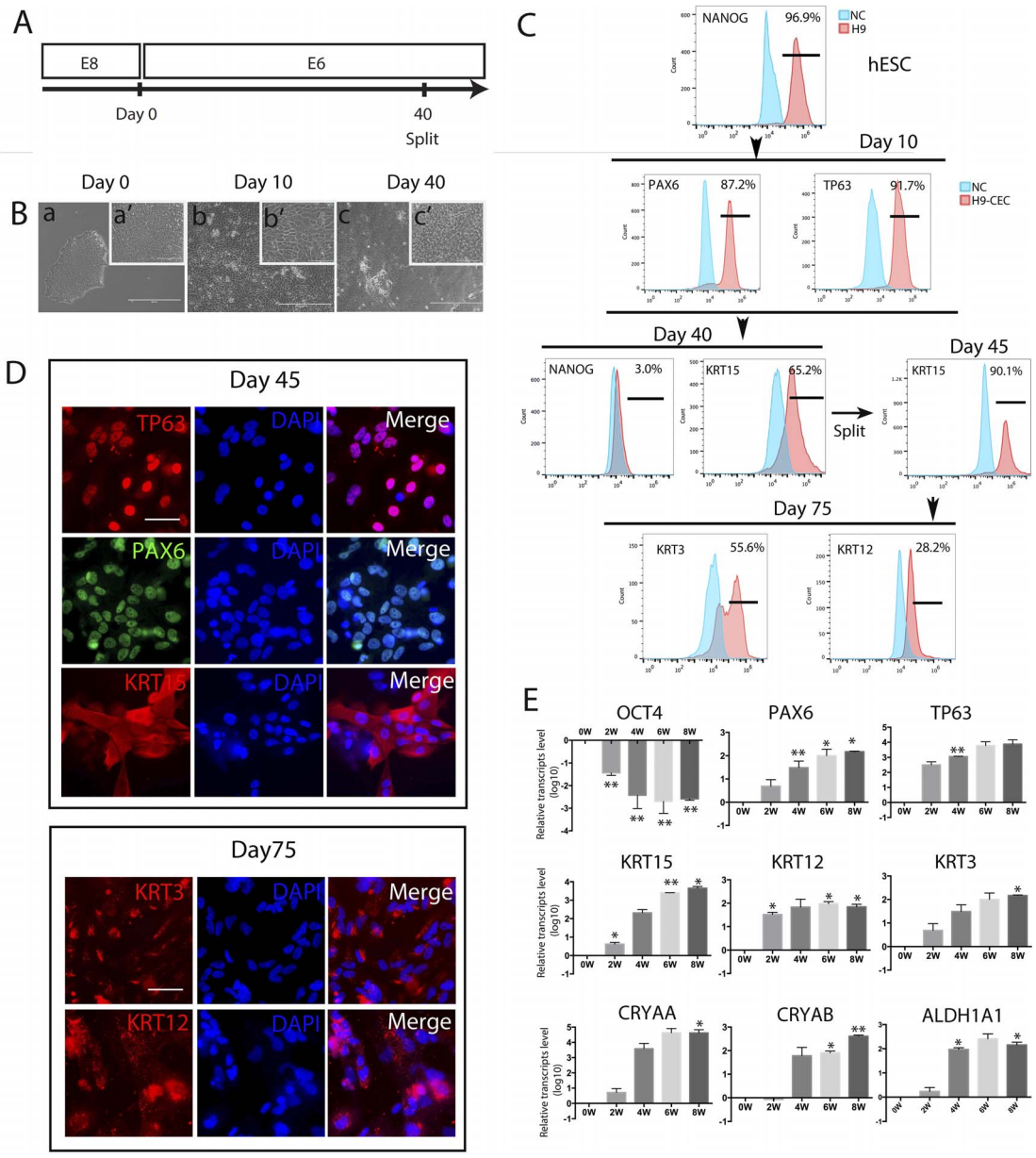

Figure 1. Generation, characterization, and differentiation efficiency of hESC-derived CEC. CEC were derived from H9 hESC, and three biological replicates were set up for each sample, and each experiment was repeated at least twice (the same hereafter unless stated otherwise). (**A**) A schematic showing the protocol for hESC differentiation into CEC in E6 with the cells split at day 40. (**B**) Morphology of the differentiated cells at days 10 and 40. *Scale bar*: 400 μm (a, b, c) and 100 μm (a′, b′, c′). (**C**) Flow cytometry analyses for the pluripotency marker NANOG, the corneal developmental markers PAX6, TP63, and KRT15, and the mature CEC markers KRT3 and KRT12 in hESC that differentiated in E6 for the designated times. (**D**) Immunostaining for TP63, PAX6, and KRT15 at day 45 of differentiation, and KRT3 and KRT12 at day 75. *Scale bar*: 50 μm for all images. (**E**) Real-time PCR analysis for expression of marker genes for pluripotency, CEC progenitors, and mature CEC, and transparency-associated genes during hESC differentiation to CEC for 8 weeks.

coated with Matrigel. After the cells reached 10% to 15% confluency, the culture medium was replaced with E6 (Invitrogen) alone (Fig. 1A), or supplemented with IWR1, A83-01, and basic fibroblast growth factor (bFGF; 3F) or 3F plus bone morphogenetic protein 4 (4F) (Supplementary Fig. S1A) to initiate CEC differentiation. Four days later, all media were replaced with E6 and followed by daily refreshment of E6 to continue the differentiation. By day 40, the cells were dissociated with EDTA/DPBS until most of the epithelial cells became round and detached (which took up to 1 hour). The dissociated cells were

harvested gently without disturbing the attached nonepithelial cells and seeded at 1:3 ratio on a new coated 6-well plate containing E6 medium and 1-μM Y27632 (Stemgent, Cambridge, MA). The cells then were maintained in E6, which was refreshed every other day.

Real-Time Polymerase Chain Reaction (PCR)

Total RNA was extracted using Trizol reagent (Ambion, Inc., Austin, TX). cDNA was synthesized with random primers and Moloney murine leukemia virus reverse transcriptase (M-MLV RT; Invitrogen) after removing genomic DNA with DNase I (Thermo Fisher Scientific, Waltham, MA). Real-time PCR was performed with the SYRB Green PCR master kit (Applied Biosystems, Foster City, CA) on a C1000 Touch Thermal Cycler (Bio-Rad Laboratories, Hercules, CA) using program: 2 minutes at 50°C, 10 minutes at 95°C, and 40 cycles of 15 seconds at 95°C and 1 minute at 60°C. Primer sequences for specific genes are presented in Supplementary Table S1. *Glyceraldehyde 3-phosphate dehydrogenase* (*GAPDH*) was tested as an endogenous reference to calculate the relative expression level of target genes. The results are displayed as relative mRNA levels.

Microarray Gene Expression Analysis

For microarray experiment, RNA was isolated from undifferentiated H9 and differentiated and harvested H9 cells for various time points (2, 4, 6, 8 weeks), using Purlink RNA mini kit (Life Technologies, Carlsbad, CA) and cDNA libraries were synthesized and processed using a single HumanHT-12 v4 Expression Beadchip in the genomics core of Faculty of Health Sciences. Further analysis was performed using Beads Studio Software (Illumina, San Diego, CA), Cluster, TreeView, and Excel software. First, we used the quantile normalization method to normalize each data point against the other intra-array samples data. The normalized dataset for CEC was filtered to remove data points with detection a P value < 0.95 in all samples. The dataset was further normalized by calculating the fold change for each probe intensity of analyzed genes, compared to the probe intensity of each gene in undifferentiated H9 cells.

Flow Cytometry Analysis

Cells in adherent culture were dissociated into single cells with 1× TrypLE and fixed by 4% paraformaldehyde (PFA) for 30 minutes at room temperature. The fixed cells were incubated in 0.1% Triton X-100 solution for 10 minutes, blocked in 5% bovine serum albumin (BSA) for 1 hour, and incubated with antibodies against NANOG (Cell Signaling Technologies), PAX6 (Invitrogen), TP63 (Boster, Pleasanton, CA) or KRT15 (Santa Cruz Biotechnology, Inc., Dallas, TX), HLA-A/B/C (ebioscience, San Diego, CA), B2M (Sigma-Aldrich Corp., St. Louis, MO) at the dilution ratio of 1:100 overnight in a cold room. The cells then were washed in cold PBS for 15 minutes twice to remove the residual antibody, and incubated for 30 minutes with secondary antibodies, for example, goat anti-mouse, goat anti-rabbit, or donkey anti-goat IgG (Invitrogen), according to the isotype of the primary antibodies. Control cells were incubated with the secondary antibody only. Cells were washed with cold PBS and analyzed on an Accuri C6 Flow Cytometer (BD Biosciences, Franklin Lakes, NJ) and the FlowJo software (Treestar, Inc., Ashland, OR).

Hematoxylin and Eosin (H&E) Staining

Recellularized DCs were embedded with paraffin and sectioned at 5 μm thickness. The paraffin-embedded DC sections were stained with H&E for 5 minutes and 30 seconds, respectively, and visualized under a light microscope (Carl Zeiss Meditec, Inc., Dublin, CA).

Immunocytochemistry

Cells were fixed with 4% PFA for 20 minutes and permeabilized with 0.1% Triton X-100 for 10 minutes. Subsequently, the cells were blocked with 5% BSA for 60 minutes and incubated with primary antibodies against PAX6 (Thermo Fisher Scientific), TP63, Ki67 (Boster), KRT19, KRT15, KRT12 or KRT3 (Santa Cruz Biotechnology, Inc.) at instructed dilutions overnight in a cold room. Cells were washed with PBS at least 3 times and 15 minutes each time before incubation with the isotype-matching secondary antibodies (all from Invitrogen). The cell nuclei were counterstained with 4, 6-diamidino-2-phenylindole (DAPI). Bright-field and fluorescent images were captured using the Carl Zeiss Axio Observer. To check the expression of CEC markers on the recellularized DC and in sections of mouse skin tissues as controls, we processed the samples the same way and incubated with antibodies against human PAX6, KRT1,

KRT10, KRT12, KRT14, KRT15, and VINCULIN (Abcam, Cambridge, United Kingdom), and mouse MHC Class I (Abcam), followed by secondary antibodies against the isotype of the primary antibodies and counterstaining with DAPI. Bright field and fluorescent images were captured with Carl Zeiss Axio observer. All primary and secondary antibodies above were used at the dilution of 1:200 and 1:1,000, respectively.

IncuCyte Life-Cell Imaging

Cell proliferation was measured on the IncuCyte Live Cell Analysis Imaging System (Essen BioScience Inc., Ann Arbor, MI). Cells were seeded in a Matrigel coated 6-well plate at 10^5 cells per well and images were captured in nine positions per well every 2 hours over a 4-day period. Proliferation was determined by calculating the total area (% confluence) occupied by cells, starting when cell confluence reached approximately 16%.

Cell Cycle Analysis

Cells were trypsinized and fixed in 70% ethanol at −20°C overnight. Fixed cells were pelleted at 250*g* for 5 minutes, then incubated with the staining solution containing 50-μg/mL Propidium iodide I (PI), 0.1-mg/mL RNase A, and 0.005% Triton X-100 in PBS, for 1 hour on ice. Then, the cells were pelleted and the supernatant was removed. PI-stained cells were suspended in 300-μL PBS and analyzed on Accuri C6 and further analyzed by ModFIT LT 5.0 software (Verity Software House, Inc., Topsham, ME).

Decellularization and Recellularization of Mouse Cornea

Under an animal use and care protocol for this and following experiments on murine eyes, approved by the University of Macau Ethics Panel, mouse corneas were isolated from the eyeballs of BALB/c mice, treated with 0.5-M sodium hydroxide for 10 minutes, washed thoroughly before they were placed at three corneas/well in a 96-well plate, and treated with ultraviolet light (UV) for 30 minutes to obtain DC. Next, three DC were recellularized in one well (96-well plate) with 2.5×10^5 either CEC derived from the GFP^+ Envy hESC or with the same number of HaCat keratinocytes. Corneas were fixed in 4% PFA overnight at 4°C for further experiments within 1 week.

Light Transmittance Through DC

The light transmission spectra of fresh mouse corneas, DC, and recellularized DC were detected via a UV-Vis-NIR spectrophotometer (Thermo Fisher Scientific) with the spectral distribution range from 400 to 800 nm. Transmittance of PBS was used to normalize the results.

Generation of *B2M*$^{-/-}$ hESC

B2M$^{-/-}$ hESC were derived from H1 hESC line using the CRISPR/Cas9 technology. *B2M*-specific sgRNA oligos were annealed and cloned into pSpCas9n(BB)-2A-GFP (PX461) and pSpCas9n(BB)-2A-Puro (PX462) V2.0 (Addgene: #48140 and #62987), respectively.[43] H1 hESC were transfected with the B2M sgRNA/nickase Cas9 pair. *B2M*$^{-/-}$ hESC were sorted via FACS and individual clones validated by genotyping and flow cytometry. Clone #1 was used in the further experiments. All procedures for handling recombinant DNA followed the NIH guidelines.

Cell Injection into the Anterior Chamber of Murine Eye

BALB/c mice were anesthetized with Tribromoethanol at 0.25 mg/g. 10^5 CECs in 2-μL PBS or PBS alone as a control was injected into the anterior chamber of the right eye of BALB/c mice using a microliter syringe. After 4 days, the mice were euthanized via CO_2 inhalation, and the injected eyeballs were isolated and fixed with 4% PFA overnight for immunohistochemistry.

Immunohistochemistry

Fixed eyeballs were dehydrated, paraffin embedded, and sectioned. Slides with the sections were stained with rabbit anti-mouse CD3 (1:500; R&D Systems, Minneapolis, MN), followed by incubation with rabbit antibody conjugated with Biotin (Jackson Laboratories, Bar Harbor, ME) was added and incubated for 1 hour. Strep-Tactin-HRP Conjugate (Bio-Rad Laboratories) at 1:500 dilution was used to amplify the signals. The substrate solution including 3,3′-diaminobensidine was added for visualization of positive cells by light microscopy.

Statistical Analysis

Data were analyzed using Prism 6 software (GraphPad Software, San Diego, CA). Statistical analysis for real-time PCR data was based on unpaired Student *t*-test with $P < 0.05$ considered

statistically significant. Microarray data were analyzed via one-way analysis.

Results

Generation of CEC from hESC in a Defined and Albumin-Free Medium E6

Recently, human iPSC were differentiated into CEC-like cells using an all-defined and serum-free corneal epithelial culture medium CnT-30, supplemented with two small chemical molecules IWP2 (an inhibitor of Wnt/β-catenin signaling) and SB-505124 (an inhibitor of TGFβ signaling), and bFGF.[17] The E8 medium developed for hPSC culture is also xeno-free, serum-free, and all defined. More importantly, it is free of albumin, a carrier for many unknown proteins, lipids, and small chemicals from the serum.[40] E6 is a derivative of E8 depleted of bFGF and TGFβ, formulated as a basal medium for hPSC differentiation. We reasoned that E6, supplemented with IWR1 (an equivalent of IWP2), A83-01 (an equivalent of SB-505124), and bFGF, might be a better choice than CnT-30 for hESC differentiation into CEC.

As shown in the schematic, H9 hESC, routinely cultured in E8 and in a Matrigel-coated plate, were allowed to differentiate in E6 (Fig. 1A), 3F, or 4F (Supplementary Fig. S1A). Four days later, all media were replaced with E6, which was refreshed daily thereafter. By day 10 of the differentiation in E6, the cells developed epithelial-like morphology and some of them possessed polygonal morphology (Fig. 1B). Flow cytometry shows that the ratios of cells positive for the ocular surface ectoderm markers PAX6 and TP63 remarkably increased to approximately 90% (Fig. 1C). Similar morphologic changes (data not shown) and $PAX6^+$ and $TP63^+$ cell ratios (Supplementary Fig. S1B) were observed with hESC lines (H1 and H9) that differentiated in E6, 3F, or 4F for 10 days. After further differentiation, the ratio of cells positive for the pluripotency marker NANOG dramatically declined from 96.9% (for hESC) to 3.0%, whereas the ratio of cells positive for the limbal stem cell marker KRT15 reached 65.2% in E6 at day 40 (Fig. 1C). Similar ratios of $KRT15^+$ cells were observed with H1 and H9 hESC that differentiated in E6, 3F, or 4F for 30 days (Supplementary Fig. S1B).

We passaged H9 hESC that differentiated in E6 for 40 days, and the $KRT15^+$ cell ratio increased to 90.1% (Fig. 1C). Immunostaining showed that the cells were positive for TP63, PAX6, and KRT15 in E6 (Fig. 1D), 3F, and 4F (Supplementary Fig. S2A). After prolonged differentiation, the cells were stained positive for two mature CEC markers KRT3 and KRT12 at day 75 in E6 (Fig. 1D) and 3F and 4F (Supplementary Fig. S2A). However, the ratios of $KRT3^+$ and $KRT12^+$ cells (detected via flow cytometry) were only 55.6% and 28.2%, respectively, among the cells differentiated in E6 (Fig. 1C). TP63, PAX6, KRT15 (at day 45), KRT3, and KRT12 (at day 75) also were detected among cells differentiated from H1, CT3, and Envy hESC lines in E6 (Supplementary Fig. S3), indicating no obvious intercell line variations.

The immunostaining data were supported by RT-qPCR analysis for expression of lineage-specific marker genes in the differentiating hESC harvested every two weeks. The expression of a pluripotency marker, *OCT4*, was down-regulated during the differentiation, whereas expression of the aforementioned CEC markers *PAX6*, *TP63*, *KRT15*, *KRT12*, and *KRT3*, as well as the transparency markers *CRYAA*, *CRYAB*, and *ALDH1A1* was up-regulated time-dependently (Fig. 1E).

It has been known that KRT15 (but not KRT3 and KRT12) also is expressed in keratinocytes.[44] To verify the quality and specificity of the antibodies for these markers, we conducted immunostaining on HaCat, a human keratinocyte line, and found that HaCat cells were indeed positive for KRT15 and negative for KRT3 and KRT12 as expected (Supplementary Fig. S2B). All data suggest that E6 alone is sufficient to allow hESC to differentiate into CEC-like cells. Thus, we used E6 throughout the study hereafter.

Gene Expression Profiling during hESC Differentiation into CEC

To gain a mechanistic insight into the cell fate specification and major signaling events involved in hESC differentiation into CEC, we performed global gene expression analysis of differentiating hESC. H9-derived CEC were harvested every 2 weeks during the differentiation and total RNA was isolated for microarray assay. The data were analyzed (Fig. 2) based on an embryonic development database LifeMap (available in the public domain at https://discovery.lifemapsc.com).

As expected, expression of pluripotency genes significantly decreased by week 2 of the differentiation and remained low. We detected elevated expres-

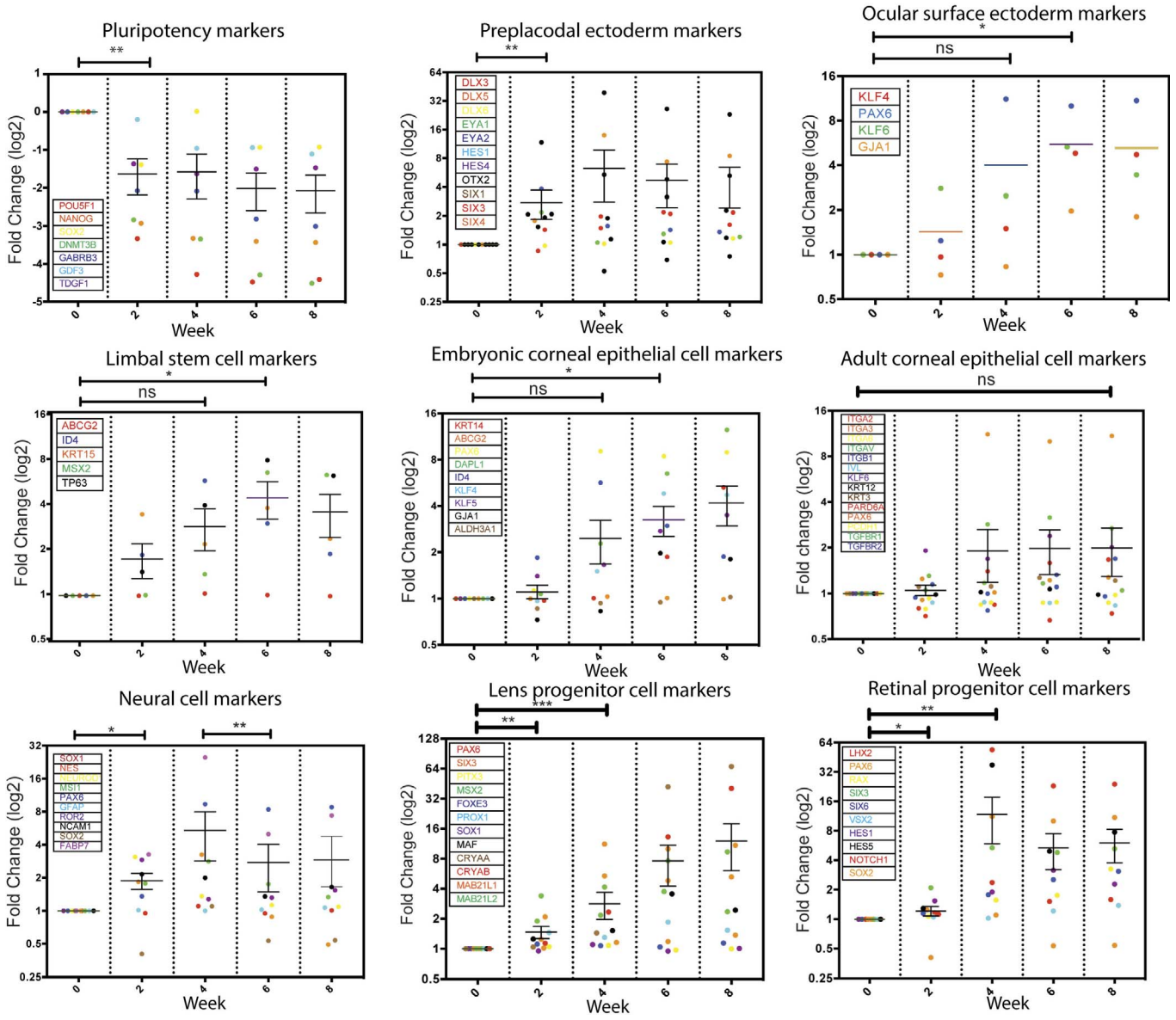

Figure 2. Dynamic gene expression profiles during hESC differentiation into CEC. Total RNA was isolated from cells differentiated from H9 hESC at various times and the global gene expression profiles were assayed via microarray. The expression of marker genes for various cell types involved in the development of the neural, corneal, and other ocular cells is displayed. Each marker gene and its corresponding data point in a relevant column scatter plot are color-matched. Statistical analysis was conducted using a paired *t*-test with two-tailed. *$P < 0.05$, **$P < 0.01$, ***$P < 0.001$, and ns: nonsignificant.

sion of preplacodal surface ectoderm markers by week 2, ocular surface ectoderm markers by week 4, and LSC and embryonic CEC markers by weeks 6 and 8, respectively. Concurrently, expression of neural and retinal markers increased by week 2 and peaked by week 4, and then gradually declined, whereas expression of lens progenitor markers increased continuously during all 8 weeks of differentiation. However, expression of adult CEC markers remained low in the differentiating cells. These data suggested that expression of the eye developmental genes, especially those related to the surface ectoderm and embryonic CEC was induced in the differentiating cells in E6, and the multistep differentiation process somehow recapitulates the embryonic processes for CEC development (Fig. 2). Pathway analysis reveals that the target genes in the Wnt and IGF signaling pathways were highly upregulated early in the differentiation then downregulated over the course of the differentiation, consistent with their

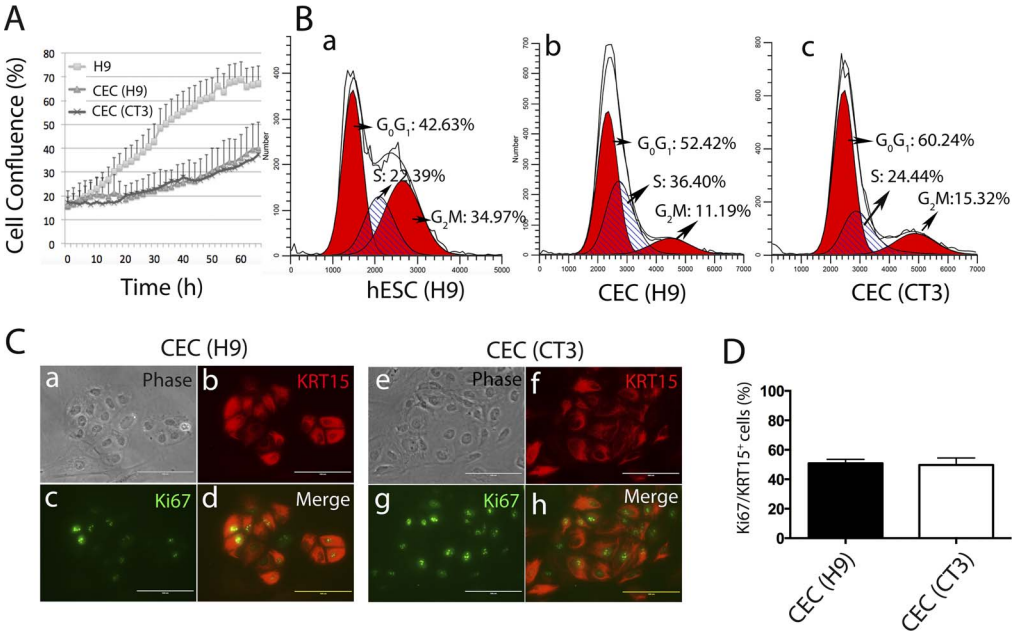

Figure 3. Proliferation of hESC-derived CEC. (A) Growth curve of hESC and hESC-derived CEC monitored on IncuCyte for 66 hours ($n = 3$). (B) Flow cytometric cell cycle analysis of PI-stained hESC and hESC-derived CEC. (C) Immunostaining for KRT15 and Ki67 on CEC. *Scale bar*: 50 μm. (D) Quantification of Ki67$^+$/KRT15$^+$ cells among CEC derived from two hESC lines H9 and CT3 ($n = 5$).

roles during CEC development[45–50] (Supplementary Fig. S4).

Proliferative Capability of hESC-Derived CEC

LSC give rise to transient amplifying cells as CEC progenitors, migrate to the basal layer of the cornea, and terminally differentiate into CEC during corneal regeneration and homeostasis.[1] One characteristic of CEC progenitors is their ability to proliferate rapidly. Thus, we analyzed whether hESC-derived CEC are proliferative. First, we monitored the growth of two independent CEC lines differentiated for approximately 50 days from H9 and CT3 hESC lines. Although both CEC lines did not proliferate as fast as the parental hESC, CEC remained proliferative at a relatively high rate during the entire 3-day observation (Fig. 3A). Second, cell cycle assay demonstrated that approximately 40% CEC were in S and G_2/M phase (Fig. 3B). Third, nearly half of KRT15$^+$ cells were Ki67$^+$ (Figs. 3C, 3D) among H9- or CT3-derived CEC. These data suggested the proliferative nature of the hESC-derived CEC.

Recellularization of Decellularized Mouse Corneas with hESC-Derived CEC

One biological hallmark of normal cornea is the transparency mainly due to the biochemical composition of corneal cells. To characterize whether ex vivo cultured or in vitro derived CEC are transparent, many tissue engraftment models use artificial matrices to seed CEC.[21–25] Here, we isolated corneas from mice and decellularized them with 0.5-M NaOH to generate DC as a corneal scaffold, and recellularizing the DC with hESC-derived CEC. Specifically, we seeded CEC that differentiated for 70 days from the GFP$^+$ Envy hESC line onto the surface of the DC (Fig. 4A). As expected, Envy hESC-derived CEC also expressed PAX6, TP63, KRT15, KRT3, and KRT12 (Supplementary Fig. S3C).

Seven days after the recellularization, we observed that the recellularized DC formed multilayered epithelium, as determined by H&E staining of a paraffinized section (Fig. 4B). Mouse DC seeded with the CEC, like the control unseeded DC, appeared a bit swollen but remained largely transparent with an underneath letter A clearly seen. However, the letter A appeared fuzzy underneath a DC seeded with human keratinocytes from the HaCat cell line (Fig. 4C). The swelling of the DC might result from the loss of the corneal endothelial cells that can pump out water from the cornea. Following dehydration in glycerol overnight, DC became crystal-clear and no longer swollen (data not shown). Furthermore, to determine the structural integrity of the CEC layers, which typically are held by desmosomes and tight junctions,[51] we tested the expression of ZO-1 in the

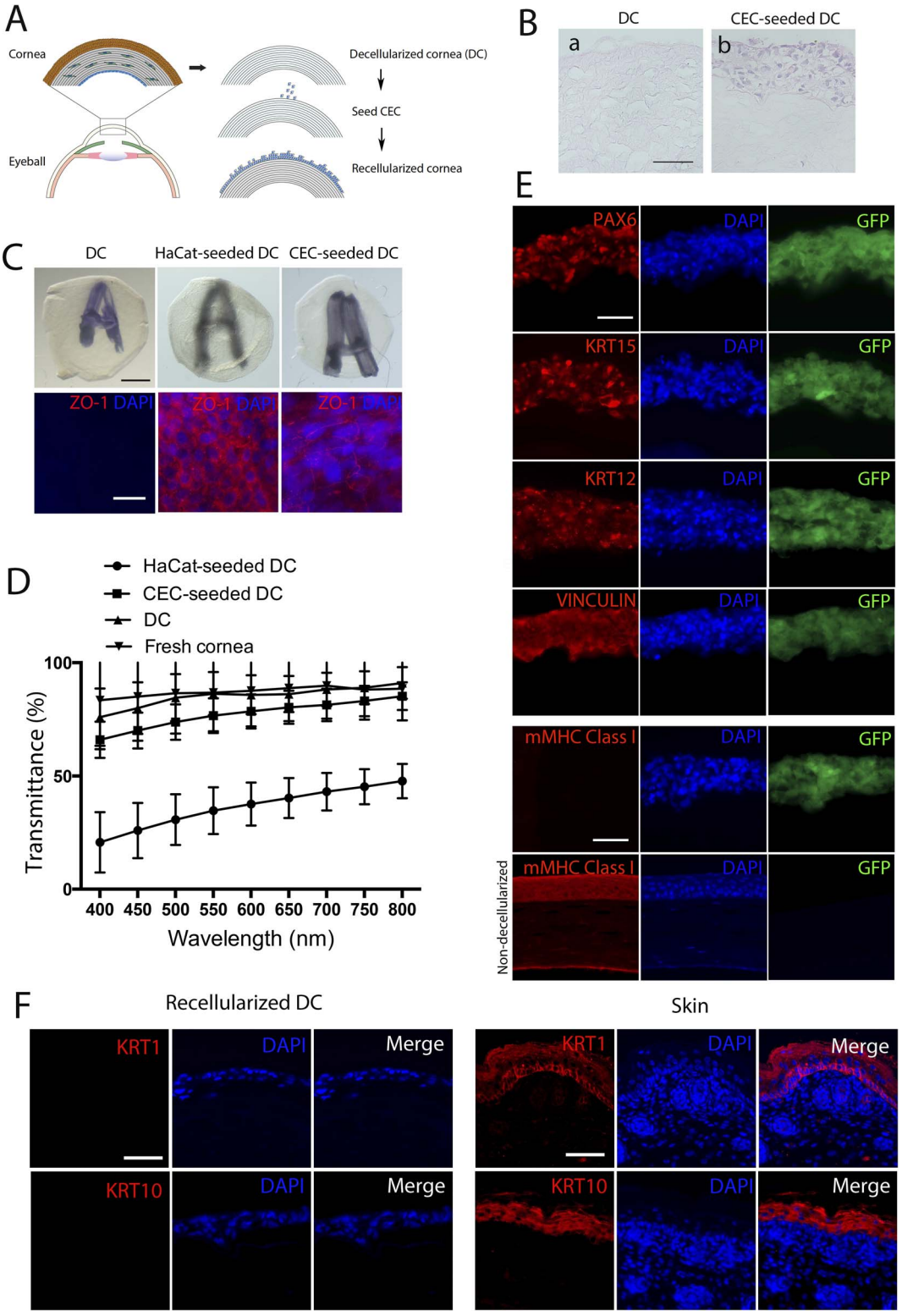

Figure 4. Recellularization of mouse DC with hESC-derived CEC. (A) A scheme for the corneal decellularization and recellularization. (B) H&E staining for determination of the multilayered structure of recellularized DC. *Scale bar*: 50 μm for both images. (C) Opacity and epithelial cell integrity of the three engineered samples DC, DC recellularized with HaCat keratinocytes, and DC recellularized with CEC. The opacity is reflected as the fuzziness of a letter A underneath the samples (*upper*), whereas the epithelial cell integrity was detected based on ZO-1 expression in the samples detected via whole-mount immunostaining. *Scale bar*: 50 μm for all. (D) The average of % →

←
transmittance of light at various wavelengths through DC, CEC- and HaCat-seeded DC ($n = 3$). (E) Fluorescent immunostaining for PAX6, KRT15, KRT12, VINCULIN, and mouse cell-specific MHC class I (mMHC-I) in CEC-seeded DC (*upper five rows*) with nondecellularized mouse cornea as a positive control for mMHC-I (*bottom row*). *Scale bar*: 50 μm for all. (F) Fluorescent immunostaining for keratinocyte markers KRT1 and KRT10 in CEC-seeded DC and sections of mouse skin tissues as a positive control. *Scale bar*: 50 μm for all.

recellularized DC using whole mount immunostaining. The tight junction marker ZO-1 was found per immunostaining to encircle CEC seeded in DC (Fig. 4C).

Consistently, transmittance of light at various wavelengths from 400 to 800 nm through the CEC-seeded DC was similar to that through the unseeded DC; however, it was 2- to 3-fold higher than that through the HaCat-seeded DC (Fig. 4D). Following immunostaining on frozen sections of the recellularized DC, all CEC seeded in the DC were positive for PAX6, KRT15, KRT12, and VINCULIN, a protein for focal cell-to-substrate attachments of spreading CEC[52] (Fig. 4E). However, it does not appear that the seeded CEC proliferated and differentiated to form multiple layers of the epithelium in DC as all were positive for KRT14, a marker for the suprabasal layers of human CEC (Supplementary Fig. S5). Furthermore, we checked expression of the keratinocyte markers KRT1 and KRT10 in the recellularized DC, which was found negative for these markers. In contrast, strong KRT1 and KRT10 expression was detected in sections of mouse skin tissues as a positive control (Fig. 4F).

To assure the absence of murine cells in the recellularized DC, we stained the sections with an antibody specific for mouse MHC class-I antigen. The CEC seeded-DC was stained negative while a normal murine cornea was positive for mouse MHC class-I molecules (Fig. 4E). Together, these data suggested that hESC-derived CEC possessed the transparency and tight junction features of corneal cells and retained CEC markers after seeding into the DC, and murine cells were totally removed from the DC.

Derivation of CEC from Low Immunogenic *B2M*$^{-/-}$ hESC

The eye generally is considered as an immune-privileged organ,[53] which supports the high success rate of corneal transplantation.[54] However, immune rejection still presents a serious threat, especially to high-risk recipients with ocular inflammation and abnormal angiogenesis.[55] Moreover, HLA class-I matching significantly increases the survival of allogeneic corneal grafts.[32,56] To minimize the potential immune rejection due to HLA mismatching, we generated a universally compatible hESC line by knocking out *B2M*, which encodes a subunit of the major histocompatibility complex I (or HLA class I in humans) on the surface of most nucleated cells. We knocked out *B2M* in both alleles in H1 hESC using the CRISPR/Cas9 technology and confirmed *B2M* mutations by Sanger sequencing of the targeted alleles (Fig. 5A). Flow cytometry analysis confirmed that B2M and HLA-A/B/C were absent from the cell surface of the *B2M*$^{-/-}$ hESC, while WT hESC expressed B2M and HLA-A/B/C (Fig. 5B).

The *B2M* knockout did not affect the pluripotency, as pluripotent markers were expressed in *B2M*$^{-/-}$ hESC (Supplementary Figs. S6A, S6B), and markers for the three germ layers expressed in differentiating *B2M*$^{-/-}$ hESC following embryoid body formation (Supplementary Fig. S6C). In addition, *B2M* knockout did not affect the CEC-generating capability, evidenced by the expression of PAX6, TP63, and KRT15 at day 45, and KRT3 and KRT12 at day 75 in CEC differentiated from the *B2M*$^{-/-}$ hESC (Fig. 5C) comparable to that in CEC from the WT H1 hESC (Supplementary Fig. S3A). More importantly, the KRT15^{+} cell ratio (49.9%) among the *B2M*$^{-/-}$ hESC that differentiated for 30 days in E6 (Supplementary Fig. S6D) is almost identical to that of the H1 WT control (49.2%; Supplementary Fig. S1B). These data suggested that the efficiency of CEC differentiation of the *B2M*$^{-/-}$ hESC was similar to that of the WT hESC.

In Vitro and In Vivo Assays on CEC Derived from *B2M*$^{-/-}$ hESC

To confirm a low immunogenicity of the *B2M*$^{-/-}$ CEC, we treated the WT and *B2M*$^{-/-}$ CEC with 100-ng/mL recombinant human interferon-γ (IFNγ), 100-ng/mL tumor necrosis factor-α (TNFα), or 100-ng/mL lipopolysaccharides (LPS) for 48 hours, respectively. After the stimulation, cells were analyzed by flow cytometry for B2M and HLA-A/B/C expression on the cell surface. WT CEC expressed B2M and HLA-A/B/C even in the absence of inflammatory factors, and the expression levels slightly increased upon the stimulations, evidenced by an increase of the

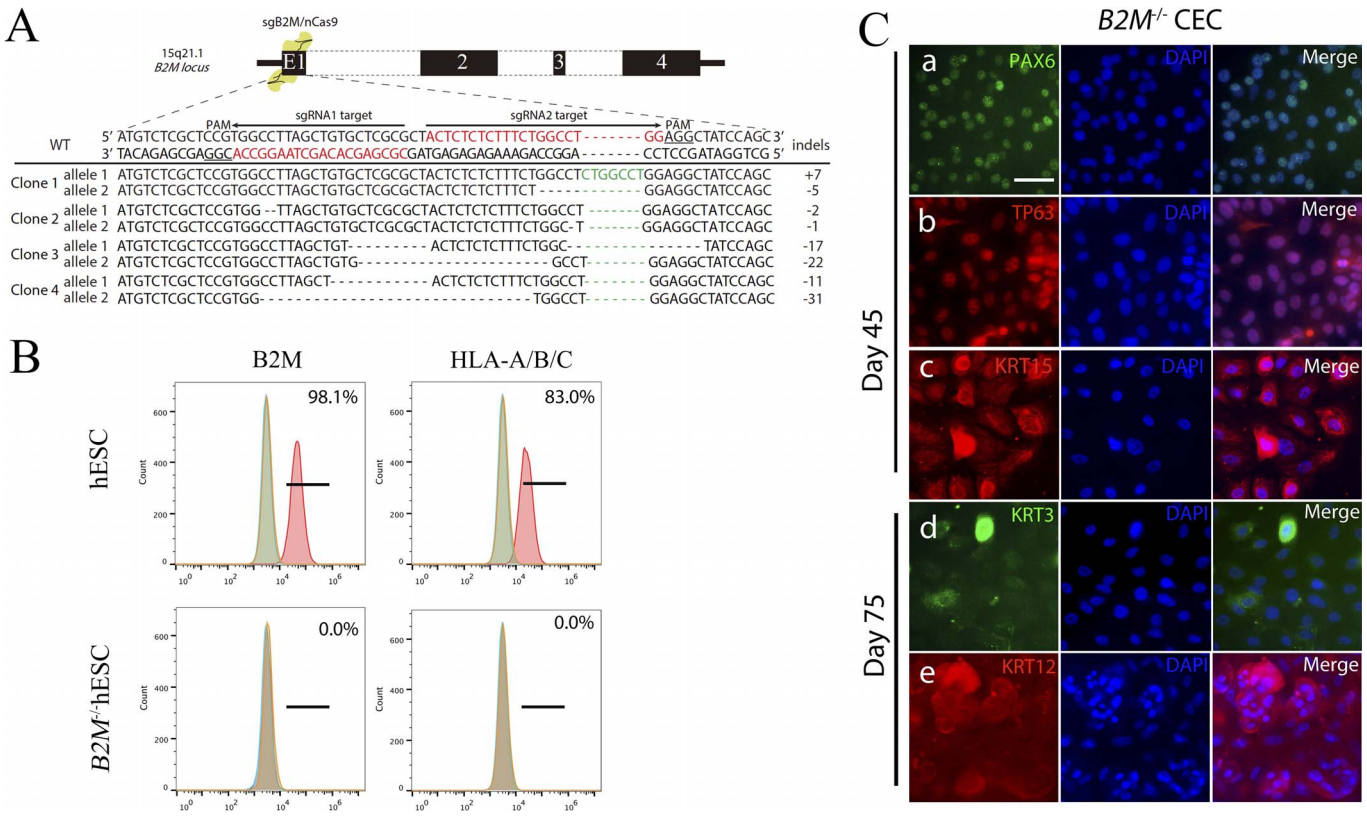

Figure 5. Generation of *B2M*$^{-/-}$ hESC and subsequent differentiation into CEC. (A) A schematic diagram for *B2M* knockout in H1 hESC using CRISPR/Cas9 and genotyping of the two alleles of *B2M* knockout clones. (B) Flow cytometry analysis for B2M and HLA-A/B/C on the cell surface of WT and *B2M*$^{-/-}$ hESC. (C) Immunostaining on cells differentiated from the *B2M*$^{-/-}$ hESC for the corneal developmental markers at day 45 and 75 of the differentiation. *Scale bar*: 50 μm.

fluorescent intensity. However, there was no expression of *B2M* and *HLA*-A/B/C in *B2M*$^{-/-}$ CEC, whether or not they were stimulated (Fig. 6).

A previous study showed that microinjection of syngeneic pancreatic islets into the anterior chamber of the murine eye caused no T-cell infiltration; however, injection with allogeneic islets resulted in an allorejection.[57] To test whether the *B2M*$^{-/-}$ CEC were less immunogenic in vivo than the WT control, we injected the cells into the anterior chamber of the murine eye to induce T lymphocyte (CD3^{+}) infiltration into the eye. Four days after injection, we observed significantly fewer CD3^{+} cells in the limbal regions of the *B2M*$^{-/-}$ CEC-injected eyeball, compared to that of the WT CEC-injected eyeball (Fig. 7). Together, these data suggested that *B2M*$^{-/-}$ CEC are less immunogenic in vitro and in vivo.

Discussion

It was reported previously that inhibition of Wnt and TGFβ signaling, in combination with activation of FGF signaling promotes CEC derivation from human iPSC in a defined medium containing human serum albumin.[17] In this study, we have shown that the basal medium E6 was sufficient to induce hESC differentiation into CEC. While an exact mechanism by which E6 differentiates hESC into CEC is not known at present, the time-course gene expression data of the differentiating cells indicated that down-regulation of Wnt/β-catenin signaling between weeks 2 and 4 of the differentiation may be important for the differentiation of CEC. Indeed, several findings previously demonstrated that inhibition of Wnt/β-catenin and TGFβ signaling is required for the development of the ocular surface ectoderm, CEC specification, and formation of the corneal epithelium.[48,49,58] Considering crosstalk between IGF-1 and Wnt/β-catenin signaling, it also is possible that the presence of insulin in E6 also has a role in modulating Wnt/β-catenin signaling through GST3β as shown in the head formation and development of ocular structures from hESC.[50]

Our protocol achieved the generation of up to 90%

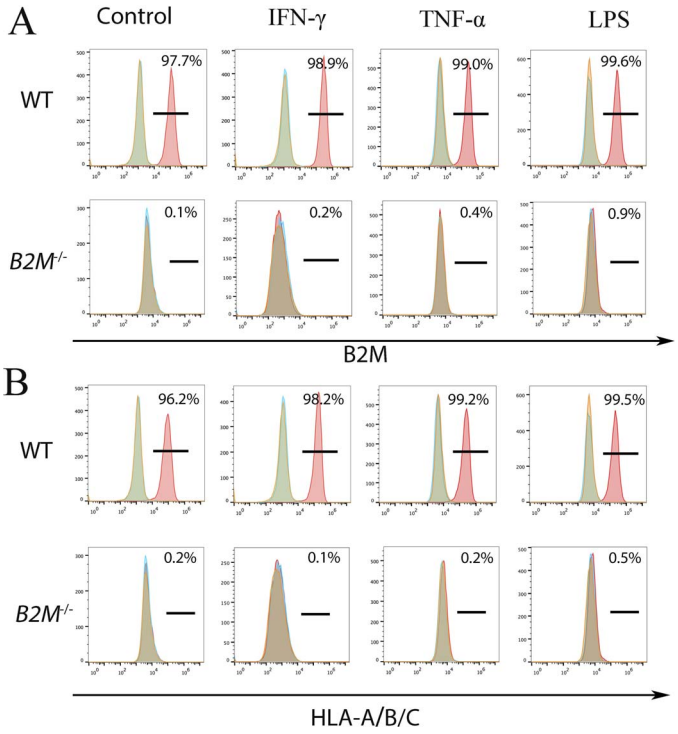

Figure 6. Expression of HLA class-I molecules on the cell surface of WT and *B2M*$^{-/-}$ H1 CEC. CEC stimulated with IFNγ (A) TNFα (B), or LPS (C) were subjected to flow cytometry for B2M and HLA-A/B/C.

KRT15^{+} cells in a two-step procedure. Expression of TP63 (92%) and PAX6 (81%), as early as day 15 of the differentiation, was followed by expression of the mature CEC markers, KRT3 and KRT12, by differentiation day 40, at similar levels to what was demonstrated previously.[17] Cell proliferation, cell cycle assays, and immunostaining for Ki67 showed a highly proliferative nature of the cells, suggesting that hESC-derived CEC in E6 may be more like CEC progenitors, including LSC and transiently amplifying cells than terminally differentiated CEC.

Animal DC recellularized with hESC-derived CEC may help address the problem of the shortage of corneal donors. Many alternative methods, such as keratoprostheses, xenografts, tissue-engineered constructs, DC, and DC recellularized with human corneal cells, have been developed. However, keratoprostheses require rigorous device maintenance, often causing wound leaks, tissue melting, and glaucoma.[59–62] Xenograft transplantation has a high rate of rejection[63] and cross-species transmission of animal viruses.[64,65] Tissue-engineered constructs lack the corneal architecture and properties of various corneal cell types. DC did not elicit any immune or inflammatory response in vivo.[27,66] Porcine DC transplanted onto damaged rabbit cornea can be repopulated by host CEC.[67] However, DC grafts cannot be properly recellularized in patients suffering from total LSCD. Thus, xenogeneic DC recellularized with hESC-derived CEC might be a viable solution.

We demonstrated that hESC-derived CEC efficiently recellularized murine DC as evidenced by stable expression of the CEC markers and formation of the tight junction barrier. Furthermore, one of the most critical features of the cornea, transparency, was clearly demonstrated on the recellularized DC. DC from larger animals, such as pig, or transparent biomaterials cellularized with hESC-derived CEC may eventually be applicable for transplantation to LSCD patients.

Another major concern for cell transplantation is immune rejection. Although the eye is considered as a relatively immune-privileged organ and the success rate of allogeneic cornea transplantation is greater than 90% in low-risk patients, immune rejection remains the leading cause of graft failure in high-risk patients. HLA antigens present on allogeneic corneas can trigger immune response in the recipient eye, leading to epithelial, chronic stromal, hyperacute, and endothelial rejections.[6,68] To our knowledge, our study for the first time addressed this problem by knocking out *B2M* in hESC before differentiating them into CEC. As expected, the *B2M*$^{-/-}$ hESC and their derived CEC lacked HLA class-I molecules on their cell surface, even after stimulation with inflammatory factors IFNγ, TNFα, and LPS. Nonetheless, no expression of HLA class-I in *B2M*$^{-/-}$ hESC-derived CEC in the presence or absence of immune stimulatory molecules suggested that the cells have lower potential for immune rejection than WT control. Indeed, much reduced lymphocyte infiltration was observed in the limbal region of mice with the anterior chamber injected with *B2M*$^{-/-}$ CEC than WT CEC, indicating a great advantage of *B2M*$^{-/-}$ CEC, especially for high-risk patients.

Conclusions

We established a simple and efficient protocol to induce hESC differentiation into CEC, recellularized DC with the CEC, and demonstrated reduced immune response of CEC differentiated from *B2M*$^{-/-}$ hESC to inflammatory factors. Some important questions remain to be addressed. First, it is critical to test the efficacy of the CEC recellularization on animal models for corneal epithelial damage and LSCD. Second, our data suggested that hESC-derived

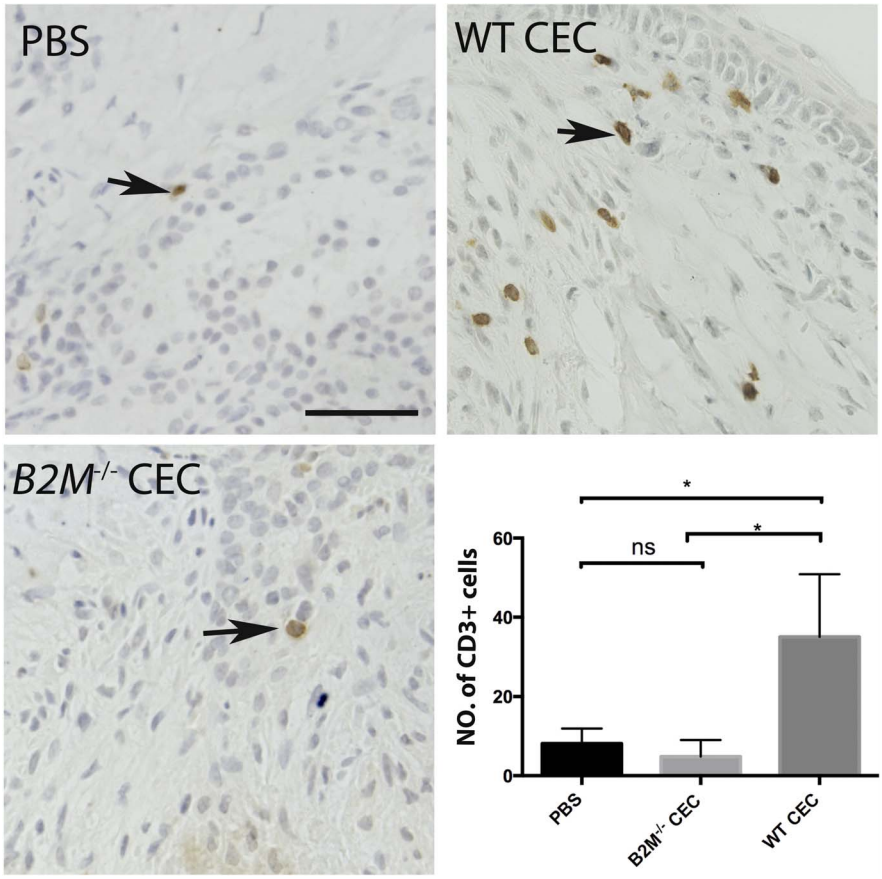

Figure 7. Immunogenicity assay on $B2M^{-/-}$ CEC in vivo. Infiltration of $CD3^+$ T cells was detected via immunohistochemistry in the limbal region of the eyeball 4 days after injection of WT or $B2M^{-/-}$ CEC or PBS into the anterior chamber of the eye of immunocompetent mice (BALB/c). The number of $CD3^+$ cells per view is displayed in a *bar chart*. PBS, $n = 4$; WT CEC, $n = 4$; $B2M^{-/-}$ CEC, $n = 3$. *Scale bar*: 100 μm. *$P < 0.05$.

CEC contained more progenitor ($KRT15^+$) CEC than mature CEC ($KRT3^+/KRT12^+$), although all CEC seeded on DC appeared $KRT12^+$ (Fig. 4E) possibly as a result of further maturation in the natural matrix for CEC. It is important to further characterize the nature of the cells before transplantation. Development of a CEC reporter line may help isolate a pure CEC population for therapeutic application and insertion of a suicide gene in the hESC before differentiation into CEC for inducible expression will eliminate any residual hESC to avoid teratoma formation. Finally, $B2M^{-/-}$ CEC, although they reduce T and B cell-mediated immune rejection, may encounter natural killer cell-mediated cytotoxicity, especially in xenogeneic animal models. In that case, transgenic expression of *HLA-E* fused with *B2M* may solve the problem as reported.[34] Addressing these remaining questions will facilitate the application of $B2M^{-/-}$ hESC-derived CEC, which could be transplanted directly or via recellularization of DC, to patients with corneal epithelial damage or LSCD.

Acknowledgments

The authors thank Single Cell and Gene Expression Analysis Core and Histopathology Core of Faculty of Health Sciences, University of Macau for services provided to this study.

Supported by University of Macau Research Committee funds MYRG #2015-00169-FHS, 2016-00070-FHS, 2017-00124-FHS and Macau Science and Technology Development Fund (FDCT) #128/2014/A3, 028/2015/A1, and 095/2017/A2 to R.X., and MYRG #2016-00249-FHS to J.W.P.

Disclosure: **J. Yang**, None; **J.W. Park**, None; **D. Zheng**, None; **R.-H. Xu**, ImStem Bioechnology Inc. (I)

References

1. Cotsarelis G, Cheng SZ, Dong G, Sun TT, Lavker RM. Existence of slow-cycling limbal epithelial basal cells that can be preferentially stimulated to proliferate: implications on epithelial stem cells. *Cell*. 1989;57:201–209.
2. Strungaru MH, Mah D, Chan CC. Focal limbal stem cell deficiency in Turner syndrome: report of two patients and review of the literature. *Cornea*. 2014;33:207–209.
3. Kim BY, Riaz KM, Bakhtiari P, et al. Medically reversible limbal stem cell disease: clinical features and management strategies. *Ophthalmology*. 2014;121:2053–2058.
4. Kolli S, Ahmad S, Lako M, Figueiredo F. Successful clinical implementation of corneal epithelial stem cell therapy for treatment of unilateral limbal stem cell deficiency. *Stem Cells*. 2010;28:597–610.
5. Dua HS, Azuara-Blanco A. Autologous limbal transplantation in patients with unilateral corneal stem cell deficiency. *Br J Ophthalmol*. 2000;84: 273–278.
6. Qazi Y, Hamrah P. Corneal allograft rejection: immunopathogenesis to therapeutics. *J Clin Cell Immunol*. 2013; 2013(suppl 9).
7. Thomson JA, Itskovitz-Eldor J, Shapiro SS, et al. Embryonic stem cell lines derived from human blastocysts. *Science*. 1998;282:1145–1147.
8. Takahashi K, Tanabe K, Ohnuki M, et al. Induction of pluripotent stem cells from adult human fibroblasts by defined factors. *Cell*. 2007; 131:861–872.
9. Yu J, Vodyanik MA, Smuga-Otto K, et al. Induced pluripotent stem cell lines derived from human somatic cells. *Science*. 2007;318:1917–1920.
10. Ahmad S, Stewart R, Yung S, et al. Differentiation of human embryonic stem cells into corneal epithelial-like cells by in vitro replication of the corneal epithelial stem cell niche. *Stem Cells*. 2007;25:1145–1155.
11. Zhu J, Zhang K, Sun Y, et al. Reconstruction of functional ocular surface by acellular porcine cornea matrix scaffold and limbal stem cells derived from human embryonic stem cells. *Tissue Engineering Part A*. 2013;19:2412–2425.
12. Brzeszczynska J, Samuel K, Greenhough S, et al. Differentiation and molecular profiling of human embryonic stem cell-derived corneal epithelial cells. *Int J Mol Med*. 2014;33:1597–1606.
13. Shalom-Feuerstein R, Serror L, De La Forest Divonne S, et al. Pluripotent stem cell model reveals essential roles for miR-450b-5p and miR-184 in embryonic corneal lineage specification. *Stem Cells*. 2012;30:898–909.
14. Hayashi R, Ishikawa Y, Ito M, et al. Generation of corneal epithelial cells from induced pluripotent stem cells derived from human dermal fibroblast and corneal limbal epithelium. *PLoS One*. 2012;7:e45435.
15. Hewitt KJ, Shamis Y, Carlson MW, et al. Three-dimensional epithelial tissues generated from human embryonic stem cells. *Tissue Engineering Part A*. 2009;15:3417–3426.
16. Hanson C, Hardarson T, Ellerstrom C, et al. Transplantation of human embryonic stem cells onto a partially wounded human cornea in vitro. *Acta Ophthalmol*. 2013;91:127–130.
17. Mikhailova A, Ilmarinen T, Uusitalo H, Skottman H. Small-molecule induction promotes corneal epithelial cell differentiation from human induced pluripotent stem cells. *Stem Cell Reports*. 2014;2:219–231.
18. Wang ZY, Zhou QJ, Duan HY, et al. Immunological properties of corneal epithelial-like cells derived from human embryonic stem cells. *Plos One*. 2016;11:e0150731.
19. Hayashi R, Ishikawa Y, Sasamoto Y, et al. Coordinated ocular development from human iPS cells and recovery of corneal function. *Nature*. 2016;531:376–380.
20. Susaimanickam PJ, Maddileti S, Pulimamidi VK, et al. Generating minicorneal organoids from human induced pluripotent stem cells. *Development*. 2017;144:2338–2351.
21. Lai JY, Wang PR, Luo LJ, Chen ST. Stabilization of collagen nanofibers with L-lysine improves the ability of carbodiimide cross-linked amniotic membranes to preserve limbal epithelial progenitor cells. *Int J Nanomedicine*. 2014;9: 5117–5130.
22. Orwin EJ, Hubel A. In vitro culture characteristics of corneal epithelial, endothelial, and keratocyte cells in a native collagen matrix. *Tissue Eng*. 2000;6:307–319.
23. Talbot M, Carrier P, Giasson CJ, et al. Autologous transplantation of rabbit limbal epithelia cultured on fibrin gels for ocular surface reconstruction. *Mol Vis*. 2006;12:65–75.

24. Sharma S, Gupta D, Mohanty S, et al. Surface-modified electrospun poly(epsilon-caprolactone) scaffold with improved optical transparency and bioactivity for damaged ocular surface reconstruction. *Invest Ophthalmol Vis Sci*. 2014;55:899–907.
25. Guan L, Ge H, Tang X, et al. Use of a silk fibroin-chitosan scaffold to construct a tissue-engineered corneal stroma. *Cells Tissues Organs*. 2013;198:190–197.
26. de la Mata A, Nieto-Miguel T, Lopez-Paniagua M, et al. Chitosan-gelatin biopolymers as carrier substrata for limbal epithelial stem cells. *J Mater Sci Mater Med*. 2013;24:2819–2829.
27. Xu YG, Xu YS, Huang C, et al. Development of a rabbit corneal equivalent using an acellular corneal matrix of a porcine substrate. *Mol Vis*. 2008;14:2180–189.
28. Yoeruek E, Bayyoud T, Maurus C, et al. Decellularization of porcine corneas and repopulation with human corneal cells for tissue-engineered xenografts. *Acta Ophthalmol*. 2012; 90:e125–e131.
29. Zhang C, Du L, Pang K, Wu X. Differentiation of human embryonic stem cells into corneal epithelial progenitor cells under defined conditions. *PLoS One*. 2017;12:e0183303.
30. Zhang Z, Niu G, Choi JS, et al. Bioengineered multilayered human corneas from discarded human corneal tissue. *Biomed Mater*. 2015;10: 035012.
31. Chen H, Wang W, Xie H, et al. A pathogenic role of IL- 17 at the early stage of corneal allograft rejection. *Transpl Immunol*. 2009;21:155–161.
32. van Essen TH, Roelen DL, Williams KA, Jager MJ. Matching for human leukocyte antigens (HLA) in corneal transplantation - to do or not to do. *Prog Retin Eye Res*. 2015;46:84–110.
33. Zheng D, Wang X, Xu RH. Concise Review: One stone for multiple birds: generating universally compatible human embryonic stem cells. *Stem Cells*. 2016;34:2269–2275.
34. Gornalusse GG, Hirata RK, Funk SE, et al. HLA-E-expressing pluripotent stem cells escape allogeneic responses and lysis by NK cells. *Nat Biotechnol*. 2017;35:765–772.
35. Wang D, Quan Y, Yan Q, Morales JE, Wetsel RA. Targeted disruption of the beta2-microglobulin gene minimizes the immunogenicity of human embryonic stem cells. *Stem Cells Transl Med*. 2015;4:1234–1245.
36. Lu P, Chen J, He L, et al. Generating hypoimmunogenic human embryonic stem cells by the disruption of beta 2-microglobulin. *Stem Cell Rev*. 2013;9:806–813.
37. Riolobos L, Hirata RK, Turtle CJ, et al. HLA engineering of human pluripotent stem cells. *Mol Ther*. 2013;21:1232–1241.
38. Feng Q, Shabrani N, Thon JN, et al. Scalable generation of universal platelets from human induced pluripotent stem cells. *Stem Cell Reports*. 2014;3:817–831.
39. Karabekian Z, Ding H, Stybayeva G, et al. HLA Class I depleted hESC as a source of hypoimmunogenic cells for tissue engineering applications. *Tissue Eng Part A*. 2015;21:2559–2571.
40. Chen G, Gulbranson DR, Hou Z, et al. Chemically defined conditions for human iPSC derivation and culture. *Nat Methods*. 2011;8:424–429.
41. Lin G, Martins-Taylor K, Xu RH. Human embryonic stem cell derivation, maintenance, and differentiation to trophoblast. *Methods Mol Biol*. 2010;636:1–24.
42. Costa M, Dottori M, Ng E, et al. The hESC line Envy expresses high levels of GFP in all differentiated progeny. *Nat Methods*. 2005;2: 259–260.
43. Ran FA, Hsu PD, Wright J, et al. Genome engineering using the CRISPR-Cas9 system. *Nat Protoc*. 2013;8:2281–2308.
44. Yang R, Zheng Y, Burrows M, et al. Generation of folliculogenic human epithelial stem cells from induced pluripotent stem cells. *Nat Commun*. 2014;5:3071.
45. Gage PJ, Qian M, Wu D, Rosenberg KI. The canonical Wnt signaling antagonist DKK2 is an essential effector of PITX2 function during normal eye development. *Dev Biol*. 2008;317: 310–324.
46. Fuhrmann S. Wnt signaling in eye organogenesis. *Organogenesis*. 2008;4:60–67.
47. Arkell RM, Tam PP. Initiating head development in mouse embryos: integrating signalling and transcriptional activity. *Open Biol*. 2012;2:120030.
48. Dupont S, Zacchigna L, Cordenonsi M, et al. Germ-layer specification and control of cell growth by ectodermin, a Smad4 ubiquitin ligase. *Cell*. 2005;121:87–99.
49. Richard-Parpaillon L, Heligon C, Chesnel F, Boujard D, Philpott A. The IGF pathway regulates head formation by inhibiting Wnt signaling in Xenopus. *Dev Biol*. 2002;244:407–417.
50. Mellough CB, Collin J, Khazim M, et al. IGF-1 Signaling plays an important role in the formation of three-dimensional laminated neural retina

and other ocular structures from Human embryonic stem cells. *Stem Cells*. 2015;33:2416–2430.
51. Sugrue SP, Zieske JD. ZO1 in corneal epithelium: association to the zonula occludens and adherens junctions. *Exp Eye Res*. 1997;64:11–20.
52. Soong HK. Vinculin in focal cell-to-substrate attachments of spreading corneal epithelial cells. *Arch Ophthalmol*. 1987;105:1129–1132.
53. Medawar PB. Immunity to homologous grafted skin; the fate of skin homografts transplanted to the brain, to subcutaneous tissue, and to the anterior chamber of the eye. *Br J Exp Pathol*. 1948;29:58–69.
54. Williams KA, Muehlberg SM, Lewis RF, Coster DJ. How successful is corneal transplantation? A report from the Australian Corneal Graft Register. *Eye (Lond)*. 1995;9(Pt 2):219–227.
55. Maguire MG, Stark WJ, Gottsch JD, et al. Risk factors for corneal graft failure and rejection in the collaborative corneal transplantation studies. Collaborative Corneal Transplantation Studies Research Group. *Ophthalmology*. 1994;101:1536–1547.
56. Reinhard T, Bohringer D, Enczmann J, et al. HLA class I and II matching improves prognosis in penetrating normal-risk keratoplasty. *Dev Ophthalmol*. 2003;36:42–49.
57. Abdulreda MH, Faleo G, Molano RD, et al. High-resolution, noninvasive longitudinal live imaging of immune responses. *Proc Natl Acad Sci U S A*. 2011;108:12863–12868.
58. Mukhopadhyay M, Gorivodsky M, Shtrom S, et al. Dkk2 plays an essential role in the corneal fate of the ocular surface epithelium. *Development*. 2006;133:2149–2154.
59. Hicks C, Crawford G, Chirila T, et al. Development and clinical assessment of an artificial cornea. *Prog Retin Eye Res*. 2000;19:149–170.
60. Netland PA, Terada H, Dohlman CH. Glaucoma associated with keratoprosthesis. *Ophthalmology*. 1998;105:751–757.
61. Chew HF, Ayres BD, Hammersmith KM et al. Boston keratoprosthesis outcomes and complications. *Cornea*. 2009;28:989–996.
62. Zerbe BL, Belin MW, Ciolino JB, Boston Type 1 Keratoprosthesis Study G. Results from the multicenter Boston Type 1 Keratoprosthesis Study. *Ophthalmology*. 2006;113:1779e1–e7.
63. Larkin DF, Williams KA. The host response in experimental corneal xenotransplantation. *Eye (Lond)*. 1995;9(Pt 2):254–260.
64. Patience C, Takeuchi Y, Weiss RA. Infection of human cells by an endogenous retrovirus of pigs. *Nat Med*. 1997;3:282–286.
65. Niu D, Wei HJ, Lin L et al. Inactivation of porcine endogenous retrovirus in pigs using CRISPR-Cas9. *Science*. 2017;357:1303–1307.
66. Hashimoto Y, Funamoto S, Sasaki S, et al. Preparation and characterization of decellularized cornea using high-hydrostatic pressurization for corneal tissue engineering. *Biomaterials*. 2010;31:3941–3948.
67. Yoeruek E, Bayyoud T, Maurus C, et al. Reconstruction of corneal stroma with decellularized porcine xenografts in a rabbit model. *Acta Ophthalmol*. 2012;90:e206–e210.
68. Panda A, Vanathi M, Kumar A, Dash Y, Priya S. Corneal graft rejection. *Surv Ophthalmol*. 2007;52:375–396.